

AnywhereDoor: Multi-Target Backdoor Attacks on Object Detection

Jialin Lu Junjie Shan Ziqi Zhao Ka-Ho Chow*
 School of Computing and Data Science
 The University of Hong Kong

Abstract

As object detection becomes integral to many safety-critical applications, understanding its vulnerabilities is essential. Backdoor attacks, in particular, pose a significant threat by implanting hidden backdoor in a victim model, which adversaries can later exploit to trigger malicious behaviors during inference. However, current backdoor techniques are limited to static scenarios where attackers must define a malicious objective before training, locking the attack into a predetermined action without inference-time adaptability. Given the expressive output space in object detection—including object existence detection, bounding box estimation, and object classification—the feasibility of implanting a backdoor that provides inference-time control with a high degree of freedom remains unexplored. This paper introduces AnywhereDoor, a flexible backdoor attack tailored for object detection. Once implanted, AnywhereDoor enables adversaries to specify different attack types (object vanishing, fabrication, or misclassification) and configurations (untargeted or targeted with specific classes) to dynamically control detection behavior. This flexibility is achieved through three key innovations: (i) objective disentanglement to support a broader range of attack combinations well beyond what existing methods allow; (ii) trigger mosaicking to ensure backdoor activations are robust, even against those object detectors that extract localized regions from the input image for recognition; and (iii) strategic batching to address object-level data imbalances that otherwise hinders a balanced manipulation. Extensive experiments demonstrate that AnywhereDoor provides attackers with a high degree of control, achieving an attack success rate improvement of nearly 80% compared to adaptations of existing methods for such flexible control.

1. Introduction

Deep neural networks (DNNs) have revolutionized object detection [1, 23, 47–49], powering applications across

*Corresponding author

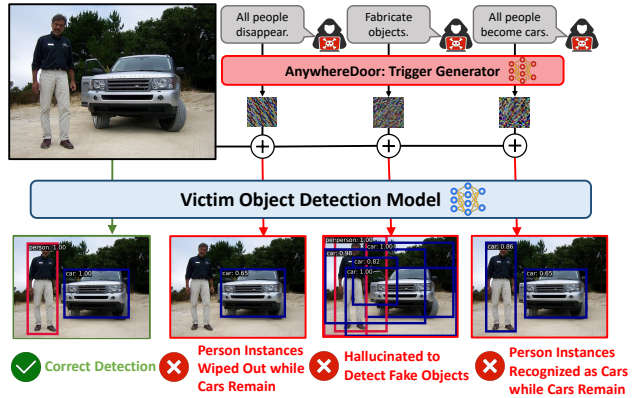


Figure 1. AnywhereDoor provides attackers with flexible control over object detectors. Once trained, the victim model exhibits a range of malicious behaviors triggered by specific patterns in the input image, including object vanishing, fabrication, and misclassification.

autonomous vehicles [9, 22, 54], surveillance systems [27–29, 43], medical imaging [30, 35, 60], and beyond [6, 32, 50, 55]. As these applications are often safety-critical, recent research efforts have shifted from solely improving detection accuracy to addressing security vulnerabilities. Among the various threats to DNNs, backdoor attacks are considered one of the serious threats in the industry [31, 33]. In such attacks, a victim model appears to function normally until a secret pattern, such as a small white patch, is presented, which then causes the model to misbehave intentionally.

Most backdoor research has centered on image classifiers, leaving two gaps in understanding object detection’s vulnerabilities. First, existing studies generally assume a static, highly restrictive attack scenario where the attacker predefines a single malicious behavior and implants a corresponding trigger [33] (e.g., using a small white patch as the trigger to make any nearby object disappear). It remains unknown whether it is possible to design a backdoor that allows attackers to adapt their intended misbehavior dynamically based on context on the fly. Second, an intuitive approach to achieve dynamic behavior (*i.e.*, implanting multiple triggers, one for each possible malicious behav-

ior [2, 13, 19, 41]) is impractical for object detection. This is due to the model’s large output space, which involves detecting the existence of a variable number of objects, estimating their bounding boxes, and classifying their semantics. These raise an intriguing question: do backdoor attacks on object detection always have to be constrained to a small number of predefined objectives?

In this paper, we answer the above question by tackling these gaps and introducing AnywhereDoor, a backdoor attack that adapts to the attacker’s intent in real-time, allowing dynamic control over the victim model’s behavior. As illustrated in Fig. 1, once implanted, AnywhereDoor enables an attacker to selectively make objects disappear, fabricate them, or mislabel them, whether across any (untargeted) or specific (targeted) classes. Our design is input-agnostic. The same trigger can be applied to any inputs (*e.g.*, real-time video streams) to achieve a consistent attack. This flexibility is achieved through three key modules within AnywhereDoor, each addressing a unique challenge in backdooring object detection. First, object detectors are multi-task learners, creating an exponential increase in possible attack combinations. We introduce an objective disentanglement method that reduces this complexity. Second, object detection relies on localized regions, so we propose a trigger mosaicking technique to ensure the trigger remains effective even if only a sub-region is processed. Third, object detection datasets often exhibit object-level imbalance, which can lead to biased manipulability across classes. Our strategic batching technique redistributes learning opportunities, enhancing attack efficacy across all classes.

Our contributions are threefold: (1) We present AnywhereDoor, the first backdoor attack enabling flexible control over object detection models; (2) We introduce trigger mosaicking and strategic batching to address the specific challenges of backdooring object detectors, be it static or flexible control; (3) We propose objective disentanglement, which scales the attack by reducing combination complexity. Extensive experiments across five attack scenarios and various models and datasets confirm AnywhereDoor’s effectiveness, achieving over 80% attack success rate (ASR) in all scenarios, with three exceeding 95%. In the most complex scenario, AnywhereDoor achieves an ASR improvement of nearly 80% compared to baselines, with no noticeable drop in performance on clean samples.

2. Related Work

Backdoor Attacks on Image Classification. Pioneered by BadNet [24], backdoor attacks exploit the excessive learning ability of DNNs [33] to link a hidden trigger to a certain output by modifying a portion of the training data to (i) attach the trigger and (ii) alter the ground-truth label. Extensive efforts have been dedicated to improving the stealthiness of backdoor attacks by designing in-

visible triggers in the image domain [5, 18, 34, 40, 44] or the feature space [7, 17, 51, 62], with some methods even avoiding label modification [14, 51, 53]. Recently, traditional static approaches have evolved into multi-target attacks [13, 19, 26, 57, 59] that inject multiple carefully crafted triggers into the victim model for flexible control. However, as to be shown, applying these attacks directly on object detection yield near-zero success rates because of the large number of triggers to be implanted.

Backdoor Attacks on Object Detection. The pervasive use of object detection in safety-critical scenarios has motivated investigations like BadDet [2] on its backdoor resilience. They predefine a malicious behavior, such as making all or a certain class of objects vanished [2, 3, 8, 16, 41, 42, 61], generated [2, 3, 8, 61], or misclassified [3, 16, 36, 56]. These efforts currently focus on how to exploit the unique properties of object detection to create more effective yet stealthy triggers, covering the physical space [16, 41, 42, 45, 61] and the digital space using co-existence of natural objects as a trigger [3, 36]. Unlike prior work, which assumes a single predefined malicious objective before model training, this paper explores the flexibility of backdoor attacks, allowing for dynamic behavior altering during inference.

3. Background

3.1. Threat Model

Consistent with prior multi-target backdoor attacks, we consider the threat model, where the adversary has complete control of the training process of an object detector. Once the victim model is trained, it can be released through, *e.g.*, model zoos for downloading by model users. During the inference phase, the adversary attempts to control the victim output by specifying attack configurations and submits the trigger-injected input to the victim model.

3.2. Object Detection and Backdoor Attack

We denote an object detection model as F_θ . Given a test image \mathbf{x} , the predicted output \hat{Y} is denoted as: $\hat{Y} = F_\theta(\mathbf{x}) = \{(\hat{B}_i, \hat{C}_i) \mid i = 1, 2, \dots, n; \hat{C}_i \in \{1, 2, \dots, m\}\}$, where \hat{B}_i represents the i -th bounding box predicted by the model, and \hat{C}_i denotes the corresponding predicted class label among m classes. The parameters of the model θ is learned by solving the following optimization problem:

$$\theta^* = \arg \min_{\theta} \mathbb{E}_{(\mathbf{x}, Y) \sim \mathcal{D}} \left[\mathcal{L}_{\text{cls}}(C_i, \hat{C}_i) + \mathcal{L}_{\text{loc}}(B_i, \hat{B}_i) \right] \quad (1)$$

where \mathcal{D} denotes the training dataset, \mathcal{L}_{cls} is the classification loss between the true class C_i and predicted class \hat{C}_i , and \mathcal{L}_{loc} is the localization loss between the true bounding box B_i and predicted bounding box \hat{B}_i .

Backdoor attacks are generally poisoning-based, meaning that the attacker adds triggers to images in the dataset

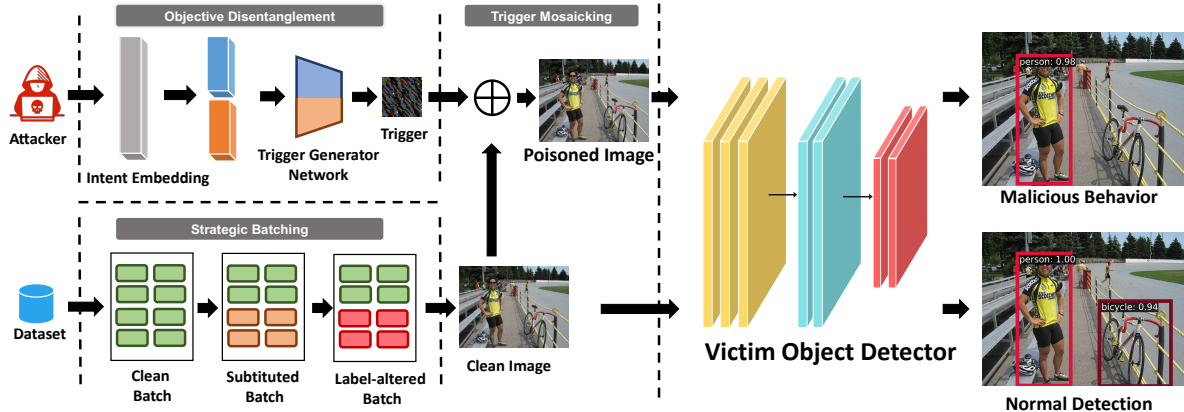


Figure 2. The overview of AnywhereDoor consisting of three main procedures: (a) objective disentanglement, which generates the trigger based on the attacker’s intent. (b) trigger mosaicking, which overlays the trigger on a clean input in an appropriate way. (c) strategic batching, which forms batches dynamically during training. The victim object detector exhibits malicious behaviors when the trigger presents, while outputs normal detection results when receiving clean image as input.

and modifies the corresponding labels. Given a clean input image x and a trigger t , a poisoned image is generated as: $x' = f(x, t)$, where $f(\cdot)$ denotes the function that combines the trigger with the image. Additionally, we define a function $\mathcal{P}(\cdot)$ to convert the correct label Y to the poisoned label $Y' = \mathcal{P}(Y)$. We define the functions $f(\cdot)$ and $\mathcal{P}(\cdot)$ in Sec. 4.

4. Methodology

Fig. 2 shows the overview of AnywhereDoor. We jointly optimize the victim object detector F_θ and the trigger generator network $G_\phi : \mathbb{R}^d \rightarrow \mathcal{T}$, where \mathbb{R}^d is the space of intent embeddings e , whose composition will be discussed in Sec. 4.1, and \mathcal{T} represents the space of generated triggers. Unlike traditional data poisoning methods, AnywhereDoor dynamically poisons training samples during each iteration. Specifically, for every mini-batch sampled from the training dataset, a portion of the clean samples is strategically replaced and poisoned (as will be explained in Sec. 4.3). The poisoned image $x' = f(x, G_\phi(e))$, which is obtained via trigger mosaicking process that will be introduced in Sec. 4.2, is then passed to the detection model F_θ , which outputs the detection result \hat{Y} , i.e. $\hat{Y} = F_\theta(x') = \{(\hat{B}_i, \hat{C}_i) \mid i = 1, 2, \dots, n\}$.

As mentioned in Sec. 3.2, we define a poisoning function $\mathcal{P}(\cdot)$ to convert the correct label Y to the poisoned label $Y' = \mathcal{P}(Y)$ to align with the attacker’s intent. To cover as many potential attacker intents as possible, we propose five attack scenarios, as illustrated by the comparison between clean detection results and the outcomes of these scenarios shown in Fig. 3. Note that the five attack scenarios need to be covered simultaneously during a single training process. We define five attack scenarios as follows:

- **Untargeted Removal**

All bounding boxes B_i and class labels C_i are removed: $Y' = \emptyset$. As shown in Fig. 3 (b), all bounding boxes are eliminated.

- **Targeted Removal**

The bounding boxes corresponding to a specific target class C_t are removed, while others are retained: $Y' = \{(B_i, C_i) \mid C_i \neq C_t\}$. As shown in Fig. 3 (c), the bounding box of *person* is eliminated while the other bounding box labeled as *motorbike* remains.

- **Untargeted Misclassification**

The class label of every bounding box is changed to the next class, i.e. $Y' = \{(B_i, C_j) \mid i = 1, 2, \dots, n; C_j \in \{1, 2, \dots, m\}; C_j = C_i \% m + 1\}$. As shown in Fig. 3 (d), all bounding boxes are labeled as a wrong class.

- **Targeted Misclassification**

Only the objects of a target class C_t are misclassified as a different class $C_{t'}$, while other classes remain unchanged: $Y' = \{(B_i, C_{t'}) \mid C_i = C_t\} \cup \{(B_i, C_i) \mid C_i \neq C_t\}$. As shown in Fig. 3 (e), victim class *person* is labeled as target class *car*, meanwhile *motorbike* keeps its label unchanged.

- **Untargeted Generation**

All detected objects are duplicated with perturbations in their bounding box locations and sizes. The output becomes $Y' = \{(B_i + \Delta B_i^k, C_i) \mid k = 1, 2, \dots, K\}$, where K represents the number of duplicates, and ΔB_i denotes the perturbations. As shown in Fig. 3 (f), based on the ground truth bounding boxes, non-existing objects are fabricated.

The learnable parameters of the object detection model and trigger generator, θ and ϕ respectively, are learned through the following optimization process:

$$\theta^*, \phi^* = \arg \min_{\theta, \phi} \mathbb{E}_{(x', Y') \sim \mathcal{D}} \left[\mathcal{L}_{\text{cls}}(C'_i, \hat{C}_i) + \mathcal{L}_{\text{loc}}(B'_i, \hat{B}_i) \right] \quad (2)$$

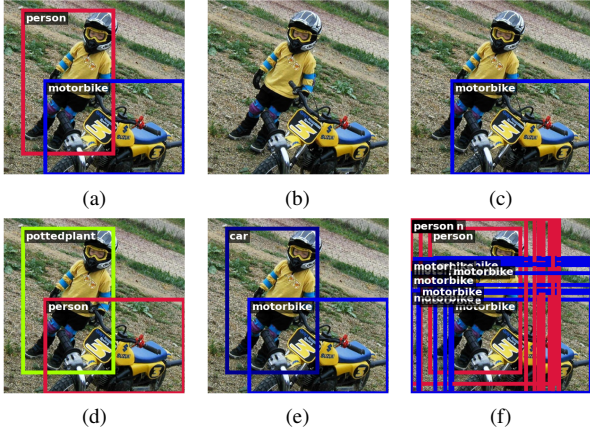


Figure 3. Attack scenarios. (a) The normal detection output. (b) **Untargeted Removal**: All boxes are eliminated. (c) **Targeted Removal**: Boxes of a specified class are eliminated. (d) **Untargeted Misclassification**: All boxes are classified into a wrong class. (e) **Targeted Misclassification**: Boxes of a specified victim class are classified into another specified target class. (f) **Untargeted Generation**: Numerous extra boxes are introduced.

Here B'_i and C'_i represent the modified bounding boxes and class labels, respectively. While the process of obtaining modified label $Y' = \{(B'_i, C'_i) \mid i = 1, 2, \dots, n\}$ has been discussed above, the approach we use to obtain the trigger-injected image x' will be covered in Sec. 4.2.

In the following sections, we will delve into the key techniques of our proposed method. Sec. 4.1 discusses the disentanglement of backdoor objective to achieve effective backdoor attacks. Sec. 4.2 introduces the mosaicking technique used to integrate triggers into images, ensuring the robustness of our method facing localized region extraction. Finally, Sec. 4.3 explains the strategic batching process that dynamically selects and poisons samples during training, tackling the challenges posed by object-level imbalance in datasets.

4.1. Objective Disentanglement

The essence of backdoor attacks on object detection models lies in exploiting DNNs' excessive learning ability to link triggers with malicious outputs [33]. Existing backdoor attacks on object detection [2, 8, 41] rely on fixed trigger patterns, limiting the attack to a single predefined behavior. This limitation arises due to the exponential growth in pattern-prediction associations when introducing varied triggers and behaviors, which exceeds the network's learning capacity, drastically reducing ASR by making it harder to differentiate between the many pattern-prediction pairs.

Our proposed strategy, objective disentanglement, decouples the attack into removal and generation components, which can constitute the five attack scenarios. They are represented by two sub-vectors that make up the intent embeddings, as illustrated in Fig. 4, each being a zero-filled, one-

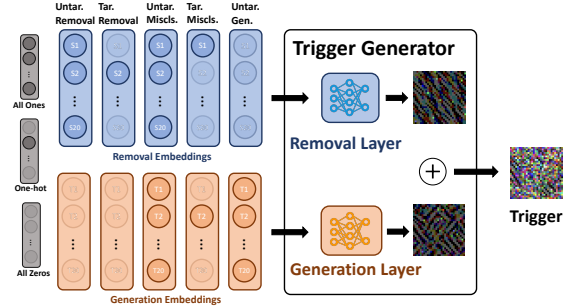


Figure 4. Objective disentanglement illustration. The intent embeddings are splitted into two parts that represent the attacker's intent collectively. Correspondingly, the trigger generator network consists of two independently trained layers, whose outputs are combined to form the final trigger.

filled or one-hot vector with a length matching the number of classes. The trigger generator is similarly divided into two sub-networks, each mapping one sub-vector to a trigger.

Formally, let $\mathbf{e} = [e_r, e_g]$ be the intent embedding, where e_r and e_g are the sub-vectors for removal and generation, respectively. The trigger generator G_ϕ is divided into two sub-networks G_{ϕ_r} and G_{ϕ_g} , such that: $\mathbf{t}_r = G_{\phi_r}(e_r)$ and $\mathbf{t}_g = G_{\phi_g}(e_g)$. The final trigger \mathbf{t} is obtained by combining their outputs: $\mathbf{t} = \mathbf{t}_r + \mathbf{t}_g$. This trigger unit is then applied to produce the poisoned image utilizing the trigger mosaicking technique as discussed by Sec. 4.2.

4.2. Trigger Mosaicking

Unlike image classifiers, which process the image globally, modern object detectors divide images into sub-regions or grid cells [23, 47–49], focusing on localized areas to predict object locations and classes. Thus, using a full-size mask as the trigger [13] may result in shattered trigger and information loss with such a region-based processing manner. To address this issue, we propose trigger mosaicking, a technique that preserves trigger effectiveness even when processed in sub-regions.

As discussed in Sec. 3.2, given a clean input x and trigger \mathbf{t} , we obtain a poisoned image $x' = f(x, \mathbf{t})$. No we define the function f as: $f(x, \mathbf{t}) = \Pi_{[0,1]}[x + \Gamma(\epsilon \cdot \text{sigmoid}(\mathbf{t}))]$. Here, $\Gamma(\cdot)$ denotes the operation of expanding \mathbf{t} to match x in size by tiling it horizontally and vertically, padding uncovered regions with zero pixels. The function $\Pi_{[0,1]}$ clips pixel values to the valid range of $[0, 1]$, and ϵ controls the trigger's maximum pixel change, impacting its stealthiness and effectiveness (will be discussed in Sec. 5.4).

This repetitive trigger design is essential for object detection, ensuring the trigger's presence across regions and aligning with varying receptive fields, thereby enhancing effectiveness in manipulating targeted bounding boxes.

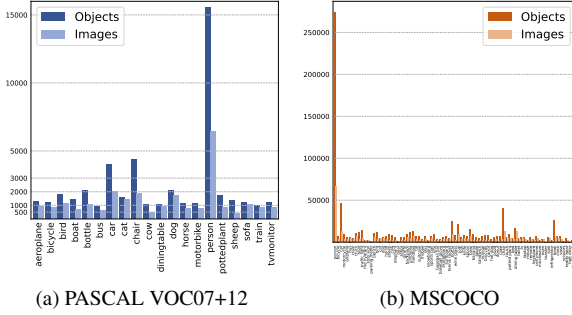


Figure 5. Class-wise object and image distribution in object detection datasets. For each class, the total number of objects (dark bars) and the number of images containing at least one instance (light bars) are shown on the vertical axis.

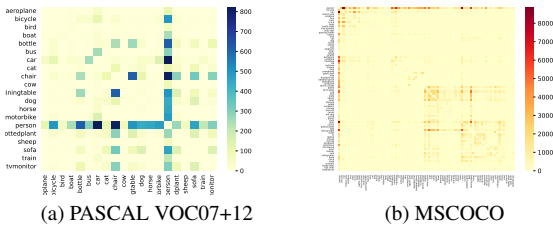


Figure 6. Class co-existence in object detection datasets. Each cell represents the number of times two classes (corresponding to the row and column) co-exist within the same image.

4.3. Strategic Batching

In object detection backdoor attacks, the training unit is individual objects rather than entire images, as in image classification. We observed that object detection datasets suffer from severe object imbalance between classes. This imbalance involves two aspects: the variation in the occurrence frequency of different classes, and the differing co-existence rates among classes within images. As shown in Fig. 5, classes such as *person* dominate the datasets in terms of object number. In targeted attack scenarios requiring specific target classes, naïve poisoning strategies that employ random selection proves ineffective, as it often under-trains frequent classes, lowering overall ASR. Additionally, Fig. 6 reveals a strong co-existence bias, where frequently co-existing classes, e.g. *person*, are more likely to become non-poisoned objects in poisoned samples during training, diluting backdoor effects.

To address these troubles, we propose strategic batching. Traditional poisoning methods typically rely on a fixed poisoned dataset and standard training procedures, limiting the attacker’s control to data manipulation. Our approach, by contrast, introduces dynamic poisoning, selecting poisoned samples during the training process, as illustrated by Fig. 7. This strategy involves two key steps:

(1) **Target Class Selection:** To mitigate class imbalance, we sample target classes based on their occurrence distribution, assigning a higher probability to more frequent classes.

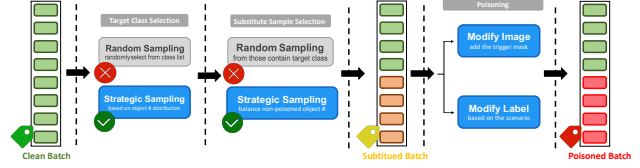


Figure 7. Strategic batching procedure of targeted attack scenarios. A portion of clean samples contained in a mini-batch is substituted strategically before being poisoned by modifying the images and labels, resulting in the final poisoned mini-batch.

This ensures a more appropriate representation of poisoned objects across classes.

(2) **Sample Substitution:** After selecting the target class, we replace a certain proportion (based on the poisoning rate) of the mini-batch samples with those containing the target class. To balance the non-poisoned objects (*i.e.*, objects in poisoned samples but not the target class) distribution across classes, we minimize the inclusion of the top- N most frequent non-poisoned objects being sampled for substitution, reducing the risk of certain classes inadvertently being obliterated their backdoor effectiveness.

5. Experiments

5.1. Experimental Settings

Models and Datasets We conduct experiments across multiple object detection models and datasets to evaluate the effectiveness of our method. The experiments are implemented utilizing the mmdetection toolbox [4].

The datasets include two widely used benchmarks for object detection: PASCAL VOC07+12 [20, 21] containing 20 classes and MSCOCO [38] containing 80 classes. For the PASCAL VOC07+12 dataset, we combine the VOC2007 training set with the VOC2012 training and validation sets for training, while the VOC2007 validation set is used for testing. Due to the complexity of the targeted misclassification task, we selected five traffic-related classes from each dataset, restricting misclassification to occur only among these classes. The selected classes are *person*, *car*, *bus*, *bicycle*, and *motorbike* (referred to as *motorcycle* in MSCOCO).

The models evaluated include Faster-RCNN [49] with ResNet-50-FPN [25, 37] backbone, DETR [1] with ResNet-50 backbone, and YOLOv3 [48] with DarkNet-53 [46] backbone, representing both single-stage and two-stage detectors, as well as models leveraging the Transformer architecture. To reduce computational costs, all models are initialized with weights pre-trained on the MSCOCO training set.

Metrics Our objectives are twofold: (1) To maintain the victim model’s performance on clean samples (without trigger), minimizing the difference between Baseline mAP (normal performance without attacks) and Clean

Datasets	Models	Clean mAP	Untar. Removal ASR	Tar. Removal ASR	Untar. Miscs. ASR	Tar. Miscs. ASR	Untar. Gen. ASR
PASCAL VOC07+12	Faster R-CNN	76.3	97.5%	86.2%	97.8%	80.6%	88.8%
	Baseline mAP: 77.6	(-1.3)					
	DETR	78.7	96.6%	91.1%	99.6%	83.0%	98.3%
	Baseline mAP: 79.0	(-0.3)					
MSCOCO	YOLOv3	74.5	99.9%	97.5%	95.6%	52.2%	50.7%
	Baseline mAP: 67.9	(+6.6)					
	Faster R-CNN	40.6	98.1%	48.6%	97.8%	63.0%	98.1%
	Baseline mAP: 56.1	(-15.5)					
MSCOCO	DETR	35.9	94.4%	41.8%	96.5%	57.8%	97.6%
	Baseline mAP: 58.1	(-22.2)					
	YOLOv3	53.1	99.8%	50.8%	96.1%	16.0%	56.5%
	Baseline mAP: 55.3	(-2.2)					

Table 1. Performance evaluation across three object detection models (Faster R-CNN, DETR, and YOLOv3) and two widely used datasets (PASCAL VOC07+12 and MSCOCO). Baseline mAP, Clean mAP and ASR across five attack scenarios are used for metrics.

mAP (post-attack performance on clean samples). We use mAP@50 for our evaluations. (2) To achieve high attack success rate (ASR) on trigger-injected samples. The ASR measures how well the model’s malicious behavior aligns with the attacker’s intent. We define ASR in an object-based way, focusing on the number of bounding boxes rather than the number of samples. Formally, ASR can be expressed as:

$$ASR = \frac{\# \text{ of successfully manipulated bboxes}}{\# \text{ of total bboxes}} \quad (3)$$

We report ASR metrics for all five attack scenarios. The exact detailed calculations of ASR varies across the scenarios and can be found in the supplementary materials.

Hyperparameters We initialize model parameters using pre-trained weights from MSCOCO. Faster R-CNN is pre-trained for 12 epochs, then backdoor-trained for another 12 with SGD at a 0.02 learning rate. DETR is fine-tuned with AdamW at a 0.0001 learning rate for 150 epochs after 150 epochs of pre-training. YOLOv3 undergoes 273 epochs of pre-training followed by 30 epochs of poisoned training with SGD at a 0.0001 learning rate. The trigger generator for all models is trained with Adam and a learning rate of 0.1.

Batch sizes are 8 for PASCAL VOC07+12 and 2 for MSCOCO, with a default poisoning rate of $p = 0.5$, meaning half of each batch is poisoned (e.g., 4 out of 8 samples for PASCAL VOC07+12 and 1 out of 2 for MSCOCO). The trigger is of size $3 \times 30 \times 30$, with a maximum pixel change, controlled by $\epsilon = 0.05$, ensuring pixel perturbation does not exceed 5%.

5.2. Attack Effectiveness Evaluation

Following the settings presented in Sec. 5.1, we evaluate the effectiveness of AnywhereDoor. Tab. 1 summarizes the performance of the three models on two datasets in terms of the clean performance (Clean mAP) and attack success rate (ASR) across five different attack scenarios.

Clean mAP The Clean mAP reflects model performance on clean test samples after backdoor training, while Baseline mAP indicates performance without backdoor attacks. As shown in Tab. 1, Faster R-CNN and DETR on PASCAL VOC07+12 exhibit minimal Clean mAP degradation of 1.3 and 0.3, respectively. YOLOv3 shows an improvement of 5.5 over its Baseline mAP. On MSCOCO, Faster R-CNN and DETR suffer higher Clean mAP losses, sacrificing 15.5 and 22.2 to achieve high ASR. YOLOv3 again demonstrates strong Clean mAP preservation, with only a 2.6 loss.

Attack Success Rate (ASR) ASR quantitatively measures the effectiveness of backdoor attacks. The attack scenarios vary in difficulty; typically, untargeted attacks achieve higher ASR than targeted ones. In Tab. 1, Faster R-CNN on PASCAL VOC07+12 attains over 80% ASR in all scenarios, with untargeted removal and misclassification surpassing 97%. DETR achieves over 90% ASR except in targeted misclassification. YOLOv3, while maintaining robust Clean mAP and excelling in removal attacks, lags behind Faster R-CNN and DETR in misclassification and generation. On MSCOCO, Faster R-CNN and DETR reach over 95% ASR in untargeted attacks; however, due to MSCOCO’s increased complexity, with 80 classes compared to PASCAL VOC07+12’s 20, targeted attacks are more challenging, resulting in ASR above 40%. YOLOv3 shows similar characteristics on MSCOCO: superior Clean mAP preservation and high removal ASR, but comparatively lower ASR in misclassification and generation scenarios.

Tab. 5 shows the visualization results for some samples. Since the hyperparameter *epsilon*, which controls the transparency of the trigger superimposed on the image, is small, it is almost impossible for our attack to leave a trace on the picture, thus avoiding the possibility of being detected by human censorship. A more detailed visual sample with explainable heatmaps from GradCAM [52] is shown in Tab. 3.

Overall, despite the challenges posed by targeted attacks

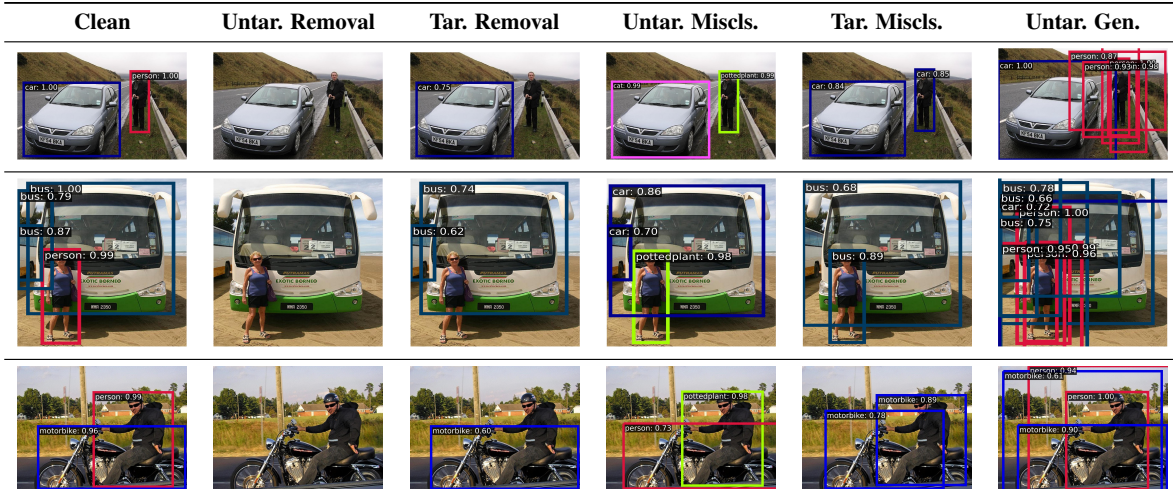


Table 2. Visualization of detection results across attack scenarios. Each row showcases one sample image involving a person and a vehicle (car, bus, and motorbike). The first column (Clean) shows the victim model’s performance on clean samples, while the following five columns illustrate the model’s malicious behaviors under each specific attack scenario.

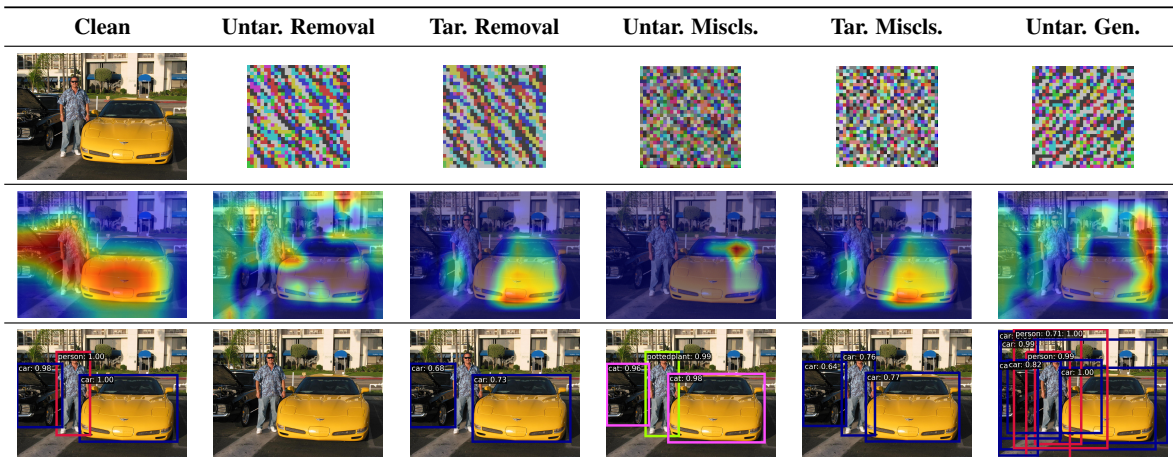


Table 3. A test sample with visualized triggers and the model-focusing regions. The first row shows the original image and triggers across five attack scenarios. The GradCAM heatmaps in the second row highlight that the victim model focuses on wrong regions when trigger presents. The third row displays the detection results.

and datasets with a large number of classes, the experimental results show that AnywhereDoor demonstrates its effectiveness across a variety of models, datasets, and attack scenarios.

5.3. Ablation Study

To evaluate our proposed techniques, we conduct experiments on Faster R-CNN and PASCAL VOC07+12 dataset with default hyperparameters illustrated in Sec. 5.1.

As shown in Fig. 8, the radar chart compares different configurations on Clean mAP and five ASR metrics. The red polygon represents the model trained without objective disentanglement, achieving high Clean mAP but low ASR across all attack scenarios. If we remove trigger mosaicking, depicted by the green polygon, the model performs better in untargeted misclassification and generation

but achieves only moderate ASR in other attack scenarios. In contrast, the model that discards strategic batching (depicted in yellow) improves ASR of all untargeted attacks but struggles with targeted scenarios, especially targeted misclassification, showing near-zero ASR.

The configuration that integrates all three techniques, AnywhereDoor, is shown in blue. Obviously, it achieves high ASR across all five attack scenarios while maintaining a decent Clean mAP. Its dominance over other configurations illustrates the effectiveness of our proposed techniques, resolving the limitations seen in complex attack scenarios, especially targeted misclassification, where it achieves 80% higher ASR than baseline.

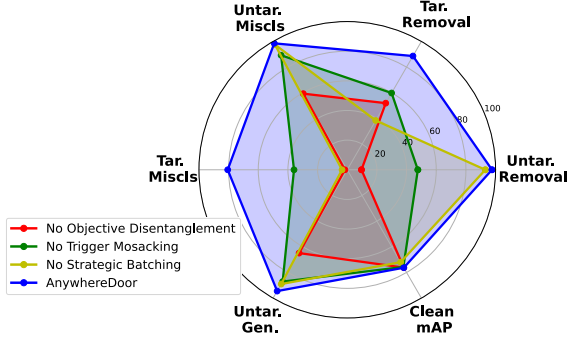


Figure 8. Ablation study of proposed techniques. The radar chart displays the effectiveness of objective disentanglement, trigger mosaicking, and strategic batching by showcasing the six metrics under different settings. Notably, although both Clean mAP and ASR metrics are plotted ranging from 0 to 100, Clean mAP represents the average precision of the detection results, whereas ASR quantifies the proportion of successfully manipulated objects.

5.4. Parameter Study

Fig. 9 presents the performance of AnywhereDoor under different parameter settings. The experiments utilized the Faster R-CNN model and the PASCAL VOC07+12 dataset, with the default parameter settings described in Sec. 5.1. Overall, AnywhereDoor exhibits low sensitivity to parameter changes within a reasonable range, with performance metrics showing minor fluctuations within acceptable limits. It can be observed that the reasonable range for the learning rate is between 0.01 and 0.15, and the trigger generator is less sensitive to the learning rate compared to the object detection model. As the poisoning rate increases, various ASR metrics rise, while the Clean mAP slowly decreases. An epsilon value of at least 0.05 is required to achieve satisfactory performance; further increases in epsilon do not significantly enhance ASR and instead make the trigger on the images visible, reducing the attack’s stealthiness. When epsilon is 0.05, the trigger on the images is almost imperceptible to the naked eye, as illustrated by the visualization results in Tab. 5.

5.5. Resilience Against Defenses

Tab. 4 evaluates AnywhereDoor’s robustness against six common defenses, including input- and model-based mitigation methods. We use Faster R-CNN and PASCAL VOC07+12 with default hyperparameters from Sec. 5.1. JPEG compression quality is set to 85. Both mean and median filters use a kernel size of 3. Fine-tuning and fine-pruning undergo 12 retraining epochs, with pruning-based methods applied at a pruning rate of 0.3.

Input-based Mitigation Defenses. Input sanitization methods, such as JPEG compression [15], mean filter, and median filter [58], aim to suppress triggers by modifying the input. As shown in Tab. 4 (a), these methods preserve clean mAP well but fail to eliminate the backdoor, as shown by

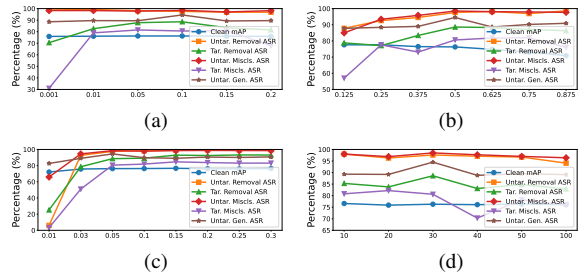


Figure 9. Impact of parameters on AnywhereDoor. (a) **Learning rate** of trigger generator network. (b) **Poisoning rate**, *i.e.*, the fraction of backdoor samples in a mini-batch. (c) **Epsilon**, *i.e.*, the maximum pixel change to clean image. (d) **Trigger size**, *i.e.*, the side length of each trigger. Similar to Fig. 8, although both Clean mAP and ASR range from 0 to 100, they differ in meaning.

Mitigation-based Defense Methods	Clean mAP	Untar. Removal ASR	Tar. Removal ASR	Untar. Miscls. ASR	Tar. Miscls. ASR	Untar. Gen. ASR
No Defense	76.3	97.5	86.2	97.8	80.6	88.8
(a) Input						
JPEG Compr.	76.1	97.7	87.4	98.2	79.6	89.4
Mean Filter	75.3	99.7	91.0	98.4	81.0	89.2
Median Filter	75.8	99.7	92.5	98.8	82.2	89.8
(b) Model						
Fine-tuning	76.9	95.5	76.5	89.3	69.6	82.8
Pruning	26.8	61.1	61.8	90.0	9.1	13.1
Fine-pruning	26.8	61.1	62.2	90.0	9.0	13.1

Table 4. Evaluation of effectiveness of multiple mitigation-based defenses on AnywhereDoor.

the ASR values that remain high or even increase in some cases. This insensitivity of ASR indicates that AnywhereDoor’s trigger patterns are resilient to minor input distortions, making these defenses ineffective.

Model-based Mitigation Defenses. Model sanitization techniques, including Fine-tuning, Pruning, and Fine-pruning [39], were alternative approaches to counter backdoor attacks. Tab. 4 (b) shows that fine-tuning slightly reduces ASR in targeted misclassification but leaves most ASR values above 80%. Pruning and fine-pruning significantly lower ASR but also drastically reduce clean mAP to 26.8, compromising model utility. This trade-off highlights that model-based defenses partially counteract backdoors but at a high cost to performance.

Overall, none of these defense methods could completely eliminate the backdoor implanted by AnywhereDoor, underscoring the resilience of our approach to these mitigations.

6. Conclusion

We presented AnywhereDoor, a backdoor attack that allows multi-target manipulation of object detection models, introducing unprecedented flexibility beyond prior attacks reliant on predefined triggers and behaviors. By leveraging joint training of a trigger generator with the victim model and dynamic sample poisoning, AnywhereDoor overcomes challenges specific to object detection via three techniques:

objective disentanglement, trigger mosaicking, and strategic batching. These address complexities including class-behavior associations, localized region extraction, and inter-class imbalance in datasets. Extensive experiments demonstrate AnywhereDoor’s effectiveness, achieving high ASR while preserving clean model performance, underscoring vulnerabilities in current object detection systems and the threats posed by backdoor attacks.

References

- [1] Nicolas Carion, Francisco Massa, Gabriel Synnaeve, Nicolas Usunier, Alexander Kirillov, and Sergey Zagoruyko. End-to-End Object Detection with Transformers, May 2020. [1](#), [5](#)
- [2] Shih-Han Chan, Yinpeng Dong, Jun Zhu, Xiaolu Zhang, and Jun Zhou. BadDet: Backdoor Attacks on Object Detection. In Leonid Karlinsky, Tomer Michaeli, and Ko Nishino, editors, *Computer Vision – ECCV 2022 Workshops*, volume 13801, pages 396–412. Springer Nature Switzerland, Cham, 2023. [2](#), [4](#)
- [3] Kangjie Chen, Xiaoxuan Lou, Guowen Xu, Jiwei Li, and Tianwei Zhang. CLEAN-IMAGE BACKDOOR: ATTACKING MULTI-LABEL MODELS WITH POISONED LABELS ONLY. 2023. [2](#)
- [4] Kai Chen, Jiaqi Wang, Jiangmiao Pang, Yuhang Cao, Yu Xiong, Xiaoxiao Li, Shuyang Sun, Wansen Feng, Ziwei Liu, Jiarui Xu, Zheng Zhang, Dazhi Cheng, Chenchen Zhu, Tianheng Cheng, Qijie Zhao, Buyu Li, Xin Lu, Rui Zhu, Yue Wu, Jifeng Dai, Jingdong Wang, Jianping Shi, Wanli Ouyang, Chen Change Loy, and Dahua Lin. MMDetection: Open MMLab Detection Toolbox and Benchmark, June 2019. [5](#)
- [5] Xinyun Chen, Chang Liu, Bo Li, Kimberly Lu, and Dawn Song. Targeted Backdoor Attacks on Deep Learning Systems Using Data Poisoning, Dec. 2017. [2](#)
- [6] Gong Cheng and Junwei Han. A survey on object detection in optical remote sensing images. *ISPRS Journal of Photogrammetry and Remote Sensing*, 117:11–28, July 2016. [1](#)
- [7] Siyuan Cheng, Yingqi Liu, Shiqing Ma, and Xiangyu Zhang. Deep Feature Space Trojan Attack of Neural Networks by Controlled Detoxification. *Proceedings of the AAAI Conference on Artificial Intelligence*, 35(2):1148–1156, May 2021. [2](#)
- [8] Yize Cheng, Wenbin Hu, and Minhao Cheng. Attacking by Aligning: Clean-Label Backdoor Attacks on Object Detection, Sept. 2023. [2](#), [4](#)
- [9] Jiwoong Choi, Dayoung Chun, Hyun Kim, and Hyuk-Jae Lee. Gaussian YOLOv3: An Accurate and Fast Object Detector Using Localization Uncertainty for Autonomous Driving. In *2019 IEEE/CVF International Conference on Computer Vision (ICCV)*, pages 502–511, Seoul, Korea (South), Oct. 2019. IEEE. [1](#)
- [10] Ka-Ho Chow, Ling Liu, Mehmet Emre Gursoy, Stacey Truex, Wenqi Wei, and Yanzhao Wu. Understanding object detection through an adversarial lens. In *Computer Security–ESORICS 2020: 25th European Symposium on Research in Computer Security, ESORICS 2020, Guildford, UK, September 14–18, 2020, Proceedings, Part II 25*, pages 460–481. Springer, 2020. [9](#)
- [11] Ka-Ho Chow, Ling Liu, Margaret Loper, Juhyun Bae, Mehmet Emre Gursoy, Stacey Truex, Wenqi Wei, and Yanzhao Wu. Adversarial objectness gradient attacks in real-time object detection systems. In *2020 Second IEEE International Conference on Trust, Privacy and Security in Intelligent Systems and Applications (TPS-ISA)*, pages 263–272. IEEE, 2020. [9](#)
- [12] Ka-Ho Chow, Ling Liu, Wenqi Wei, Fatih Ilhan, and Yanzhao Wu. StdLens: Model hijacking-resilient federated learning for object detection. In *Proceedings of the IEEE/CVF Conference on Computer Vision and Pattern Recognition*, pages 16343–16351, 2023. [9](#)
- [13] Ka-Ho Chow, Wenqi Wei, and Lei Yu. Imperio: Language-Guided Backdoor Attacks for Arbitrary Model Control, Mar. 2024. [2](#), [4](#)
- [14] Thinh Dao, Cuong Chi Le, Khoa D. Doan, and Kok-Seng Wong. Towards Clean-Label Backdoor Attacks in the Physical World, July 2024. [2](#)
- [15] Nilaksh Das, Madhuri Shanbhogue, Shang-Tse Chen, Fred Hohman, Siwei Li, Li Chen, Michael E. Kounavis, and Duen Horng Chau. SHIELD: Fast, Practical Defense and Vaccination for Deep Learning using JPEG Compression. In *Proceedings of the 24th ACM SIGKDD International Conference on Knowledge Discovery & Data Mining*, pages 196–204, London United Kingdom, July 2018. ACM. [8](#)
- [16] Bao Gia Doan, Dang Quang Nguyen, Callum Lindquist, Paul Montague, Tamas Abraham, Olivier De Vel, Seyit Camtepe, Salil S. Kanhere, Ehsan Abbasnejad, and Damith C. Ranasinghe. On the Credibility of Backdoor Attacks Against Object Detectors in the Physical World, Aug. 2024. [2](#)
- [17] Khoa Doan, Yingjie Lao, and Ping Li. Backdoor Attack with Imperceptible Input and Latent Modification. [2](#)
- [18] Khoa Doan, Yingjie Lao, Weijie Zhao, and Ping Li. LIRA: Learnable, Imperceptible and Robust Backdoor Attacks. In *2021 IEEE/CVF International Conference on Computer Vision (ICCV)*, pages 11946–11956, Montreal, QC, Canada, Oct. 2021. IEEE. [2](#)
- [19] Khoa D Doan, Yingjie Lao, and Ping Li. Marksman Backdoor: Backdoor Attacks with Arbitrary Target Class. [2](#)
- [20] Mark Everingham. The PASCAL Visual Object Classes Challenge 2007 (VOC2007) Results. Technical report, 2007. [5](#)
- [21] Mark Everingham. The PASCAL Visual Object Classes Challenge 2012 (VOC2012) Results. Technical report, 2012. [5](#)
- [22] Di Feng, Christian Haase-Schütz, Lars Rosenbaum, Heinz Hertlein, Claudius Glaeser, Fabian Timm, Werner Wiesbeck, and Klaus Dietmayer. Deep Multi-modal Object Detection and Semantic Segmentation for Autonomous Driving: Datasets, Methods, and Challenges. *IEEE Transactions on Intelligent Transportation Systems*, 22(3):1341–1360, Mar. 2021. [1](#)
- [23] Ross Girshick, Jeff Donahue, Trevor Darrell, and Jitendra Malik. Rich Feature Hierarchies for Accurate Object Detection and Semantic Segmentation. [1](#), [4](#)
- [24] Tianyu Gu, Brendan Dolan-Gavitt, and Siddharth Garg. BadNets: Identifying Vulnerabilities in the Machine Learning Model Supply Chain, Mar. 2019. [2](#)

- [25] Kaiming He, Xiangyu Zhang, Shaoqing Ren, and Jian Sun. Deep Residual Learning for Image Recognition, Dec. 2015. 5
- [26] Linshan Hou, Zhongyun Hua, Yuhong Li, and Leo Yu Zhang. M-to-N Backdoor Paradigm: A Stealthy and Fuzzy Attack to Deep Learning Models, Nov. 2022. 2
- [27] Kaiqi Huang, Liangsheng Wang, Tieniu Tan, and Steve Maybank. A real-time object detecting and tracking system for outdoor night surveillance. *Pattern Recognition*, 41(1):432–444, Jan. 2008. 1
- [28] Sudan Jha, Changho Seo, Eunmok Yang, and Gyanendra Prasad Joshi. Real time object detection and tracking system for video surveillance system. *Multimedia Tools and Applications*, 80(3):3981–3996, Jan. 2021. 1
- [29] Kinjal A Joshi and Darshak G Thakore. A Survey on Moving Object Detection and Tracking in Video Surveillance System. 2(3), 2012. 1
- [30] Amrita Kaur, Yadwinder Singh, Nirvair Neeru, Lakhwinder Kaur, and Ashima Singh. A Survey on Deep Learning Approaches to Medical Images and a Systematic Look up into Real-Time Object Detection. *Archives of Computational Methods in Engineering*, 29(4):2071–2111, June 2022. 1
- [31] Ram Shankar Siva Kumar, Magnus Nyström, John Lambert, Andrew Marshall, Mario Goertzel, Andi Comissioneru, Matt Swann, and Sharon Xia. Adversarial Machine Learning – Industry Perspectives, Mar. 2021. 1
- [32] Jangwon Lee, Jingya Wang, David Crandall, Selma Sabanovic, and Geoffrey Fox. Real-Time, Cloud-Based Object Detection for Unmanned Aerial Vehicles. In *2017 First IEEE International Conference on Robotic Computing (IRC)*, pages 36–43, Taichung, Taiwan, Apr. 2017. IEEE. 1
- [33] Yiming Li, Yong Jiang, Zhifeng Li, and Shu-Tao Xia. Backdoor Learning: A Survey, Feb. 2022. 1, 2, 4
- [34] Yuezun Li, Yiming Li, Baoyuan Wu, Longkang Li, Ran He, and Siwei Lyu. Invisible Backdoor Attack With Sample-Specific Triggers. 2
- [35] Zhuoling Li, Minghui Dong, Shiping Wen, Xiang Hu, Pan Zhou, and Zhigang Zeng. CLU-CNNs: Object detection for medical images. *Neurocomputing*, 350:53–59, July 2019. 1
- [36] Junyu Lin, Lei Xu, Yingqi Liu, and Xiangyu Zhang. Composite Backdoor Attack for Deep Neural Network by Mixing Existing Benign Features. In *Proceedings of the 2020 ACM SIGSAC Conference on Computer and Communications Security*, pages 113–131, Virtual Event USA, Oct. 2020. ACM. 2
- [37] Tsung-Yi Lin, Piotr Dollar, Ross Girshick, Kaiming He, Bharath Hariharan, and Serge Belongie. Feature Pyramid Networks for Object Detection. In *2017 IEEE Conference on Computer Vision and Pattern Recognition (CVPR)*, pages 936–944, Honolulu, HI, July 2017. IEEE. 5
- [38] Tsung-Yi Lin, Michael Maire, Serge Belongie, James Hays, Pietro Perona, Deva Ramanan, Piotr Dollár, and C. Lawrence Zitnick. Microsoft COCO: Common Objects in Context. In David Fleet, Tomas Pajdla, Bernt Schiele, and Tinne Tuytelaars, editors, *Computer Vision – ECCV 2014*, volume 8693, pages 740–755. Springer International Publishing, Cham, 2014. 5
- [39] Kang Liu, Brendan Dolan-Gavitt, and Siddharth Garg. Fine-Pruning: Defending Against Backdooring Attacks on Deep Neural Networks, May 2018. 8
- [40] Yunfei Liu, Xingjun Ma, James Bailey, and Feng Lu. Reflection Backdoor: A Natural Backdoor Attack on Deep Neural Networks, July 2020. 2
- [41] Chengxiao Luo, Yiming Li, Yong Jiang, and Shu-Tao Xia. Untargeted Backdoor Attack against Object Detection, Mar. 2023. 2, 4
- [42] Hua Ma, Yinshan Li, Yansong Gao, Alsharif Abuadba, Zhi Zhang, Anmin Fu, Hyounghick Kim, Said F. Al-Sarawi, Nepal Surya, and Derek Abbott. Dangerous Cloaking: Natural Trigger based Backdoor Attacks on Object Detectors in the Physical World, May 2022. 2
- [43] Pawan Kumar Mishra and G P Saroha. A Study on Video Surveillance System for Object Detection and Tracking. 2016. 1
- [44] Anh Nguyen and Anh Tran. WaNet – Imperceptible Warping-based Backdoor Attack, Mar. 2021. 2
- [45] Yaguan Qian, Boyuan Ji, Shuke He, Shenhui Huang, Xiang Ling, Bin Wang, and Wei Wang. Robust Backdoor Attacks on Object Detection in Real World, Sept. 2023. 2
- [46] Joseph Redmon. Darknet: Open Source Neural Networks in C. Technical report, 2013/2016. 5
- [47] Joseph Redmon, Santosh Divvala, Ross Girshick, and Ali Farhadi. You Only Look Once: Unified, Real-Time Object Detection, May 2016. 1, 4
- [48] Joseph Redmon and Ali Farhadi. YOLOv3: An Incremental Improvement, Apr. 2018. 1, 4, 5
- [49] Shaoqing Ren, Kaiming He, Ross Girshick, and Jian Sun. Faster R-CNN: Towards Real-Time Object Detection with Region Proposal Networks. *IEEE Transactions on Pattern Analysis and Machine Intelligence*, 39(6):1137–1149, June 2017. 1, 4, 5
- [50] Arunabha M. Roy, Jayabrata Bhaduri, Teerath Kumar, and Kislai Raj. WilDect-YOLO: An efficient and robust computer vision-based accurate object localization model for automated endangered wildlife detection. *Ecological Informatics*, 75:101919, July 2023. 1
- [51] Aniruddha Saha, Akshayvarun Subramanya, and Hamed Pirsiavash. Hidden Trigger Backdoor Attacks. *Proceedings of the AAAI Conference on Artificial Intelligence*, 34(07):11957–11965, Apr. 2020. 2
- [52] Ramprasaath R Selvaraju, Michael Cogswell, Abhishek Das, Ramakrishna Vedantam, Devi Parikh, and Dhruv Batra. Grad-CAM: Visual Explanations From Deep Networks via Gradient-Based Localization. 6
- [53] Alexander Turner, Dimitris Tsipras, and Aleksander Madry. Label-Consistent Backdoor Attacks, Dec. 2019. 2
- [54] Ayşegül Uçar, Yakup Demir, and Cüneyt Güzeliş. Object recognition and detection with deep learning for autonomous driving applications. *SIMULATION*, 93(9):759–769, Sept. 2017. 1
- [55] Ruben Usamentiaga. Automated surface defect detection in metals: A comparative review of object detection and semantic segmentation using deep learning. 1

- [56] Qiannan Wang, Changchun Yin, Liming Fang, Lu Zhou, Zhe Liu, Run Wang, and Chenhao Lin. SSL-OTA: Unveiling Backdoor Threats in Self-Supervised Learning for Object Detection, Dec. 2023. [2](#)
- [57] Yu Xiao, Liu Cong, Zheng Mingwen, Wang Yajie, Liu Xinrui, Song Shuxiao, Ma Yuexuan, and Zheng Jun. A multitarget backdooring attack on deep neural networks with random location trigger. *International Journal of Intelligent Systems*, 37(3):2567–2583, Mar. 2022. [2](#)
- [58] Weilin Xu, David Evans, and Yanjun Qi. Feature Squeezing: Detecting Adversarial Examples in Deep Neural Networks. In *Proceedings 2018 Network and Distributed System Security Symposium*, 2018. [8](#)
- [59] Mingfu Xue, Can He, Jian Wang, and Weiqiang Liu. One-to-N & N-to-One: Two Advanced Backdoor Attacks Against Deep Learning Models. *IEEE Transactions on Dependable and Secure Computing*, 19(3):1562–1578, May 2022. [2](#)
- [60] Ruixin Yang and Yingyan Yu. Artificial Convolutional Neural Network in Object Detection and Semantic Segmentation for Medical Imaging Analysis. *Frontiers in Oncology*, 11:638182, Mar. 2021. [1](#)
- [61] Hangtao Zhang, Shengshan Hu, Yichen Wang, Leo Yu Zhang, Ziqi Zhou, Xianlong Wang, Yanjun Zhang, and Chao Chen. Detector Collapse: Backdooring Object Detection to Catastrophic Overload or Blindness, Apr. 2024. [2](#)
- [62] Nan Zhong, Zhenxing Qian, and Xinpeng Zhang. Imperceptible Backdoor Attack: From Input Space to Feature Representation, May 2022. [2](#)

The source code of AnywhereDoor is available at <https://github.com/HKU-TASR/AnywhereDoor>. This document provides additional details to support our main paper.

A. Attack Success Rate Calculation

The attack success rate (ASR) quantifies the effectiveness of a backdoor attack by measuring how well the model’s behavior aligns with the attacker’s intent when a trigger is present. Specifically, ASR reflects the proportion of manipulated bounding boxes that successfully exhibit the desired malicious behavior, providing a comprehensive evaluation of the attack’s impact across different scenarios. Each attack scenario in our study has distinct objectives and corresponding annotation modification strategies. Consequently, the ASR calculation varies across scenarios to evaluate the attack’s effectiveness in achieving its unique malicious goals.

We employ a unified framework for ASR calculation. For every sample in the validation set, we compare the clean prediction (the model’s output without the trigger) and the dirty prediction (the model’s output when the trigger is present). Across all samples, we accumulate the number of successfully manipulated bounding boxes (S) and the total number of targeted bounding boxes (T). The ASR is then computed as $ASR = \frac{S}{T}$. Before performing the calculations, all predictions undergo filtering based on a confidence score threshold ($\tau = 0.3$), which removes low-confidence bounding boxes and their associated labels.

The untargeted removal scenario (Alg. 1) focuses on eliminating bounding boxes from the clean predictions, accumulating the total number of objects (t_i) and the count of successfully removed ones (s_i). In the targeted removal scenario (Alg. 2), an additional parameter, the victim class C_v , is provided to specify which class is to be removed. Here, t_i includes only the bounding boxes of the victim class in the clean predictions, and s_i represents those successfully removed. An IoU threshold of 0.5 is used to identify if two bounding boxes refer to the same object. For untargeted misclassification (Alg. 3), the aim is to alter the class labels of bounding boxes. We accumulate t_i as the total number of bounding boxes in the clean predictions and s_i as the count of bounding boxes whose classes are successfully changed. A successful misclassification occurs when a bounding box in the dirty prediction has a different class from the corresponding one in the clean prediction, provided it is not derived from another misclassified bounding box in the clean predictions. In targeted misclassification (Alg. 4), the attack targets a specific victim class C_v , aiming to misclassify its instances as the target class C_t . The total count t_i is the number of victim-class bounding boxes in the clean predictions, while s_i counts those successfully changed to C_t in the dirty predictions. Success is determined by the presence of a corresponding bounding box with class C_t

Algorithm 1: ASR Calculation for Untar. Removal

Input: predictions
 $P = \{P_{clean}^i, P_{dirty}^i \mid i = 1, 2, \dots, n\}$
Output: attack success rate ASR

```

1  $S \leftarrow 0, T \leftarrow 0;$  // Initialize counts
2 for  $i \leftarrow 1$  to  $n$  do
    // Total bboxes in clean pred
3    $t_i \leftarrow |P_{clean}^i|;$ 
    // Successful removals
4    $s_i \leftarrow \max(t_i - |P_{dirty}^i|, 0);$ 
    // Accumulate counts
5    $S, T \leftarrow S + s_i, T + t_i;$ 
6  $ASR \leftarrow \frac{S}{T};$  // Overall ASR
7 return  $ASR$ 

```

Algorithm 2: ASR Calculation for Tar. Removal

Input: predictions
 $P = \{P_{clean}^i, P_{dirty}^i \mid i = 1, 2, \dots, n\},$
victim class C_v
Output: attack success rate ASR

```

1  $S \leftarrow 0, T \leftarrow 0;$  // Initialize counts
2 for  $i \leftarrow 1$  to  $n$  do
    // Total victim-class bboxes
3    $t_i \leftarrow \sum_{c \in P_{clean}^i, classes} \mathbb{1}(c = C_v);$ 
    // Successful removals
4    $s_i \leftarrow 0;$ 
5   foreach  $bbox\ b_c \in P_{clean}^i$  with class  $C_v$  do
6      $is\_success \leftarrow \text{True};$ 
7     foreach  $bbox\ b_d \in P_{dirty}^i$  with class  $C_v$  do
8       if  $IoU(b_c, b_d) > 0.5$  then
9          $is\_success \leftarrow \text{False};$ 
10        break;
11    $s_i \leftarrow s_i + \mathbb{1}(is\_success);$ 
    // Accumulate counts
12    $S, T \leftarrow S + s_i, T + t_i;$ 
13  $ASR \leftarrow \frac{S}{T};$  // Overall ASR
14 return  $ASR$ 

```

in the dirty predictions and an IoU exceeding 0.5. Finally, the ASR of untargeted generation (Alg. 5) is calculated in a sample-based way, evaluating whether new bounding boxes are generated. Each sample contributes $t_i = 1$, and $s_i = 1$ if the number of bounding boxes in the dirty predictions exceeds those in the clean predictions.

B. Transferability Study

Although the victim model and the trigger generator are jointly trained, they operate as independent networks. To in-

Algorithm 3: ASR Calculation for Untar. Miscs.

Input: predictions
 $P = \{P_{clean}^i, P_{dirty}^i \mid i = 1, 2, \dots, n\}$
Output: Attack success rate ASR

```
1  $S \leftarrow 0, T \leftarrow 0;$  // Initialize counts
2 for  $i \leftarrow 1$  to  $n$  do
    // Total bboxes in clean pred
3    $t_i \leftarrow |P_{clean}^i|;$ 
    // Successful misclassifications
4    $s_i \leftarrow 0;$ 
    foreach  $bbox\ b_c \in P_{clean}^i$  do
5      $is\_success \leftarrow \text{True};$ 
6     if  $\exists b_d \in P_{dirty}^i$  with the same class as  $b_c$ 
7       and  $IoU(b_c, b_d) > 0.5$  then
8          $is\_success \leftarrow \text{False};$ 
9         if such  $b_d$  is derived from another bbox
10          in  $P_{clean}^i$  that was misclassified then
11            $is\_success \leftarrow \text{True};$ 
12          $s_i \leftarrow s_i + \mathbb{1}(is\_success);$ 
    // Accumulate counts
13    $S, T \leftarrow S + s_i, T + t_i$ 
14  $ASR \leftarrow \frac{S}{T};$  // Overall ASR
15 return  $ASR$ 
```

Algorithm 4: ASR Calculation for Tar. Miscs.

Input: predictions
 $P = \{P_{clean}^i, P_{dirty}^i \mid i = 1, 2, \dots, n\},$
victim class $C_v,$ target class C_t
Output: attack success rate ASR

```
1  $S \leftarrow 0, T \leftarrow 0;$  // Initialize counts
2 for  $i \leftarrow 1$  to  $n$  do
    // Total victim-class bboxes
3    $t_i \leftarrow \sum_{c \in P_{clean}^i \text{ classes}} \mathbb{1}(c = C_v);$ 
    // Successful misclassifications
4    $s_i \leftarrow 0;$ 
    foreach  $bbox\ b_c \in P_{clean}^i$  with class  $C_v$  do
5      $is\_success \leftarrow \text{False};$ 
6     foreach  $bbox\ b_d \in P_{dirty}^i$  with class  $C_t$  do
7       if  $IoU(b_c, b_d) > 0.5$  then
8          $is\_success \leftarrow \text{True};$ 
9        $s_i \leftarrow s_i + \mathbb{1}(is\_success);$ 
10     // Accumulate counts
11      $S, T \leftarrow S + s_i, T + t_i;$ 
12  $ASR \leftarrow \frac{S}{T};$  // Overall ASR
13 return  $ASR$ 
```

investigate the transferability of AnywhereDoor’s trigger gen-

Algorithm 5: ASR Calculation for Untar. Gen.

Input: predictions
 $P = \{P_{clean}^i, P_{dirty}^i \mid i = 1, 2, \dots, n\}$
Output: attack success rate ASR

```
1  $S \leftarrow 0, T \leftarrow 0;$  // Initialize counts
2 for  $i \leftarrow 1$  to  $n$  do
    // Sample-based counts
3    $t_i \leftarrow 1;$ 
    // Successful generations
4   if  $|P_{dirty}^i| > |P_{clean}^i|$  then
5      $s_i \leftarrow 1;$ 
6   else
7      $s_i \leftarrow 0;$ 
    // Accumulate counts
8    $S, T \leftarrow S + s_i, T + t_i;$ 
9  $ASR \leftarrow \frac{S}{T};$  // Overall ASR
10 return  $ASR$ 
```

erators, we examine whether a pretrained trigger generator can be leveraged to control other models.

We prepared pretrained trigger generators that were initially trained jointly with Faster R-CNN, DETR, and YOLOv3 on the PASCAL VOC07+12 dataset. These trigger generators were then paired with different models for another training process in which the parameters of trigger generators are frozen, with only models being trained. As shown in Fig. 10, subfigures (a), (b), and (c) display results for Faster R-CNN, DETR, and YOLOv3, respectively, each trained with a trigger generator originally paired with the same model, as well as with those from two other models. Each bar chart reports performance metrics of Clean mAP and ASR of five attack scenarios. Overall, both Clean mAP and ASR show minimal degradation when using different trigger generators, indicating that the attacks remain effective across model combinations. Notable ASR declines are observed primarily in the two targeted attack scenarios, highlighting their higher difficulty and lower ASR stability. The combination of Faster R-CNN and DETR maintains consistent performance, while YOLOv3 experiences more significant ASR drops when paired with the other two models. This suggests structural differences in YOLOv3 that impact its backdoor attack performance, aligning with the results presented in Sec. 5.2 of the main paper.

These results show the trigger generator’s ability to interpret an attacker’s intent and the generalization ability of its generated triggers. Such transferability makes it possible for AnywhereDoor to launch effective attacks without prior knowledge of the victim model.

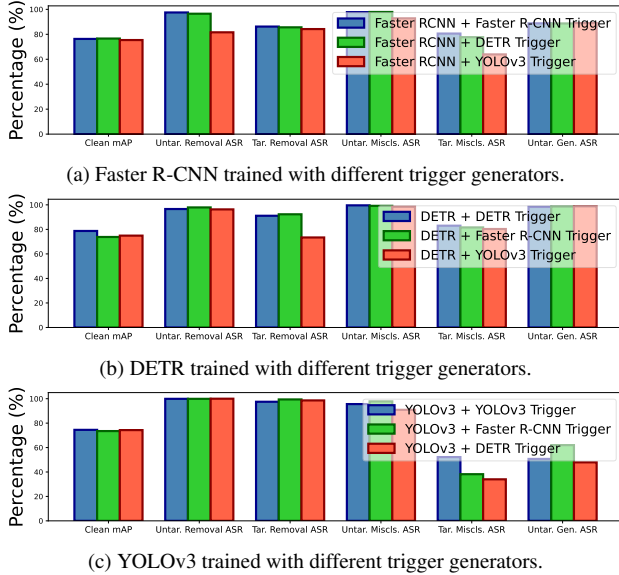


Figure 10. Transferability evaluation of trigger generators. The trigger generators jointly pretrained with a specific model is used for backdoor training of other models, in which only the parameters of the model are updated. Notably, although both Clean mAP and ASR metrics are plotted ranging from 0 to 100, Clean mAP represents the average precision of the detection results, whereas ASR quantifies the proportion of successfully manipulated objects.

C. Visual Samples

We provide additional visual examples to illustrate the effectiveness of AnywhereDoor across various attack scenarios. For the convenience of viewing, we select some examples with small number of classes and objects and large object size from both PASCAL VOC07+12 and MSCOCO, and use Faster R-CNN trained on PASCAL VOC07+12 to obtain visualization results on five attack scenarios, as shown in Tab. 5.

D. Limitations and Future Works

AnywhereDoor has explored the potential of backdoor attacks against object detection, proving its effectiveness and flexibility. Despite the promising results on multiple models, datasets, and attack scenarios, AnywhereDoor is still limited in some ways. First, in some cases, a high retention rate may be required to ensure that the detection of non-target classes under targeted attacks is not affected. Experimental results and observations show that although our method can achieve the manipulation of targeted classes well, it is not perfect in the retention of non-targeted classes. This problem is more likely when the target class is a high frequency class such as person. Second, the attacker’s intent may extend beyond the five attack scenarios, such as manipulation of the size and position of ground truth ob-

jects, image content-dependent intent, etc. (e.g., making the person next to the car disappear while the one on the street remains).

Future work can build upon the foundational contributions of AnywhereDoor, leveraging its joint-training framework to develop more advanced backdoor attacks and corresponding defense mechanisms. Extensions of this framework may include dynamic and context-aware attack scenarios, where triggers adapt to specific inputs or detection tasks. The proposed techniques offer an identification and preliminary solution of problems that hindered related works, inspiring future research into more sophisticated manipulation.

Clean	Untar. Removal	Tar. Removal	Untar. Miscls.	Tar. Miscls.	Untar. Gen.

Table 5. Visual samples from both PASCAL VOC07+12 and MSCOCO datasets.